

THE OFFICIAL MAGAZINE OF THE OCEANOGRAPHY SOCIETY

# Oceanography

## CITATION

St. Laurent, L., and S. Merrifield. 2017. Measurements of near-surface turbulence and mixing from autonomous ocean gliders. *Oceanography* 30(2):116–125, <https://doi.org/10.5670/oceanog.2017.231>.

## DOI

<https://doi.org/10.5670/oceanog.2017.231>

## COPYRIGHT

This article has been published in *Oceanography*, Volume 30, Number 2, a quarterly journal of The Oceanography Society. Copyright 2017 by The Oceanography Society. All rights reserved.

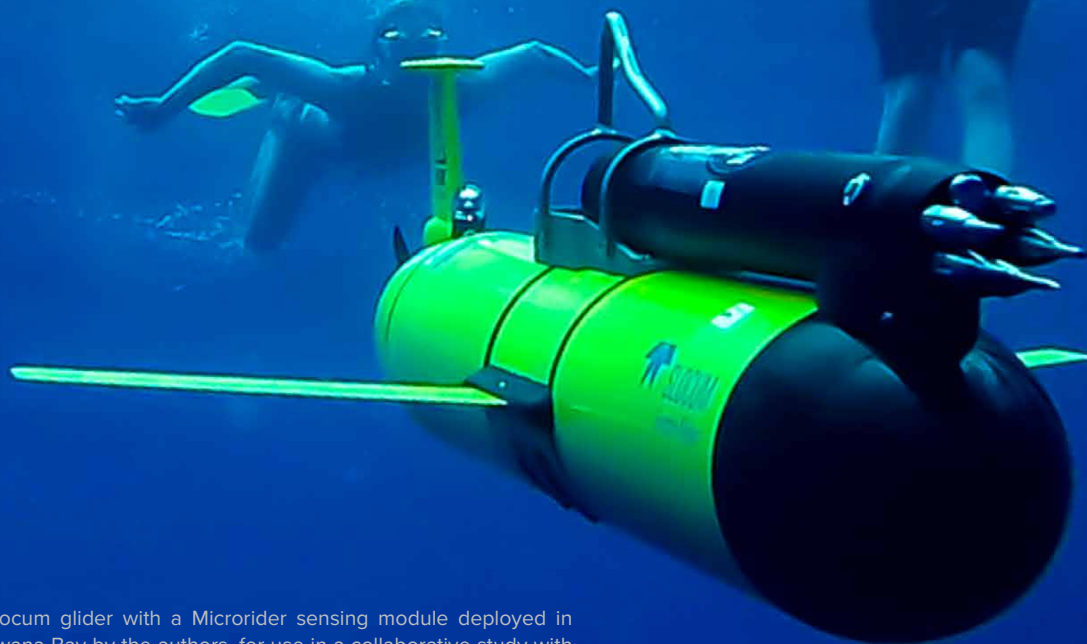
## USAGE

Permission is granted to copy this article for use in teaching and research. Republication, systematic reproduction, or collective redistribution of any portion of this article by photocopy machine, reposting, or other means is permitted only with the approval of The Oceanography Society. Send all correspondence to: [info@tos.org](mailto:info@tos.org) or The Oceanography Society, PO Box 1931, Rockville, MD 20849-1931, USA.



# Measurements of Near-Surface Turbulence and Mixing from Autonomous Ocean Gliders

By Louis St. Laurent and Sophia Merrifield



A Slocum glider with a Microrider sensing module deployed in Sodwana Bay by the authors, for use in a collaborative study with researchers (seen swimming) at the University of KwaZulu-Natal. Photo courtesy of Sean Whelan (WHOI)



**ABSTRACT.** As autonomous sampling technologies have matured, ocean sensing concepts with long histories have migrated from their traditional ship-based roots to new platforms. Here, we discuss the case of ocean microstructure sensing, which provides the basis for direct measurement of small-scale turbulence processes that lead to mixing and buoyancy flux. Due to their hydrodynamic design, gliders are an optimal platform for microstructure sensing. A buoyancy-driven glider can profile through the ocean with minimal vibrational noise, a common limitation of turbulence measurements from other platforms. Moreover, gliders collect uncontaminated data during both descents and ascents, permitting collection of near-surface measurements unattainable from ship-based sensing. Persistence and the capability to sample in sea states not feasible for deck-based operations make glider-based microstructure sampling a profoundly valuable innovation. Data from two recent studies illustrate the novel aspects of glider-based turbulence sensing. Surface stable layers, characteristic of conditions with incoming solar radiation and weak winds, exemplify a phenomenon not easily sampled with ship-based methods. In the North Atlantic, dissipation rate measurements in these layers revealed unexpected turbulent mixing during times of peak warming, when enhanced stratification in a thin layer led to an internal wave mode that received energy from the deeper internal wave field of the thermocline. Hundreds of profiles were obtained in the Bay of Bengal through a barrier layer that separates a strongly turbulent surface layer from a surprisingly quiescent interior just 20 m below. These studies demonstrate the utility of buoyancy-driven gliders for collecting oceanic turbulence measurements.

## INTRODUCTION

Direct in situ measurements of ocean turbulence have more than a 50-year history, starting with the seminal work of Grant et al. (1962). These measurements resolve the Kolmogorov scale: the scale at which the molecular viscosity of seawater balances the inertial forces of small vortices. The term “microstructure” is used to describe measurements of thermodynamic properties (e.g., velocity and temperature) at scales ranging from the Kolmogorov to those two orders of magnitude larger. For typical open-ocean conditions, this range is roughly 1 cm to 1 m. Scales exceeding these by several orders of magnitude (say, 1 m to 1,000 m) are termed “finestructure,” and characterize the motions of internal waves, intrusions, and other buoyancy anomalies associated with a range of processes.

To characterize oceanic microstructure properties requires precise measurements

of environmental flow. In the case of most ocean observational methods, the act of the measurement itself disturbs the flow at the Kolmogorov scale. Vibrational energy inherent in most ship-based measurement platforms overwhelms the signals of environmental turbulence, making an assessment of turbulence levels impossible. Due to these difficulties, many studies have focused on features of finestructure (which are much easier to measure) to draw inferences about microstructure. These methodologies typically involve measurements of shear (e.g., Kunze et al., 1990) and Thorpe scales [Thorpe, 1977]), and have varying levels of success in predicting turbulence levels and mixing rates (e.g., Mater et al., 2015). In general, no generalized finestructure parameterization has been identified, or likely will be, as the complexities of turbulence and ocean flow dynamics cannot

be entirely described by any subset of easily measurable parameters. Thus, the art of ocean microstructure measurement has remained in demand.

The methodology for computing the dissipation rate from airfoils has a long history that is described in detail in the literature (Lueck et al., 2002, and Lueck, 2003, provide comprehensive reviews). We focus our discussion here on estimation of the turbulent kinetic energy dissipation rate ( $\epsilon$ ), which quantifies the loss of kinetic energy in a fluid to molecular viscosity ( $\nu$ ). The turbulent kinetic energy dissipation rate is defined as

$$\epsilon = \nu \overline{\left( \frac{\partial u_i}{\partial x_j} + \frac{\partial u_j}{\partial x_i} \right)^2},$$

where the quantity in parentheses is the nine-component rate-of-strain tensor. In practice, our estimate is achieved through the measurement of sub-centimeter-scale vertical shear ( $\partial u / \partial z$ ) using airfoil probes (Lueck, 2003). We then invoke isotropy relations (Hinze, 1975) to reduce the nine-component rate-of-strain tensor to a single microscale shear component such that

$$\epsilon = \left( \frac{15}{2} \right) \nu \overline{\left( \frac{\partial u}{\partial z} \right)^2}.$$

A contemporary innovation involves the concurrent use of high-frequency motion sensing through multi-axis analog accelerometers. Using co-spectral analysis, we remove the platform-induced vibrations from the probe records using the method of Goodman et al. (2006). Typically, this correction applies to frequencies between about 10 Hz and 60 Hz. In the resulting “clean” shear spectra, coherent vibrational energy between the profiler platform and the shear records has been removed. As described by Wolk et al. (2009), this method allows us to measure dissipation rates as

low as about  $5 \times 10^{-11} \text{ W kg}^{-1}$ .

To estimate the dissipation rate from the cleaned spectra, we follow the spectral analysis procedure described by Gregg (1999). In practice, the microstructure records, collected at 512 Hz, were examined in 2,048-element windows over which a 1,024-element fast Fourier transform (FFT) was employed. Adjacent 1,024-element bins are treated using a Hanning window employed with 50% overlap. For the typical fall-speed of  $0.75 \text{ m s}^{-1}$ , this analysis results in spectral variance estimates at the 1.5 m depth intervals of each microstructure shear record. The limits of integration are taken from the lowest wavenumber to an upper wavenumber cutoff calculated as either 100 cycles per meter (cpm) or a lesser wavenumber representing the transition between the dissipative subrange and the portion of the high-wavenumber spectrum dominated by electronic noise. In practice, the noise-limited wavenumber nearly always applies. This cutoff wavenumber is found through identifying the corresponding root of the fifth order polynomial fit to the spectral curve. No corrections are applied to the shear spectra, as the inertial subrange and dissipative roll-off are always well resolved in these data. Dual shear probes are always used, and the dissipation rate reported is typically the mean of the independently estimated dissipation rates from each probe signal.

As a measure of fidelity, spectra are compared to the canonical spectral form derived by Nasmyth (1970) for the calculated value of the dissipation rate. Measured spectra generally show good agreement with Nasmyth. Cases where the measured spectra deviate substantially are not included in the dissipation estimates. Finally, we combine the CTD data with the dissipation estimates, computing the Ozmidov wavenumber as  $(N^3/\epsilon)^{1/2}$  (Thorpe, 2007), where  $N$  is the buoyancy frequency ( $N = \sqrt{(\partial b/\partial z)}$ ), and  $b$  is the buoyancy as calculated from the density of seawater). As the Ozmidov wavenumber corresponds to the lowest wavenumber for the dissipation integral,

we re-examine the dissipation estimate by integrating each Nasmyth spectrum from its associated Ozmidov wavenumber to infinity. This process allows us to examine the uncertainty caused by missing variance in the data spectral estimates, both at the lower and upper ends of the spectrum. Cases where the resulting estimate of integrated variance differs by more than 10% from the data estimate are flagged. These cases represent less than 0.1% of all estimates, and are not included in further estimates.

Traditionally, microstructure measurements have been made from ship-operated platforms of two types: towed systems that are generally run along constant depth transects, and vertical dropsondes that profile in depth. Towed systems are pulled at high tension, which leads to transmission of ship-based motions to the profiling platform. To prevent this noise from degrading the microstructure measurements, towed profiling systems are typically very large, so their large inertial mass damps ship- and platform-originating vibrational energy. Paka et al. (1999), Lueck et al. (2002), and Dillon et al. (2003) describe examples of such towed platforms.

Dropsonde-type instruments are often referred to as vertical profilers. The most common forms are loosely tethered to a ship-based winch. Free fall is achieved by spooling slack tether at about twice the fall rate of the profiler as it descends. A variant of this concept, in which buoyancy is added to the profiler and slack tether is predeployed to depth, allows for upward, free-ascent sampling of microstructure. While a slack tether greatly reduces the transmission of sea-surface-induced vibrational energy to the profiling system, the added drag of a tether adds its own issues to the flight dynamics of the system. Furthermore, the issues associated with tether management are considerable, especially if sampling to depths greater than several hundred meters.

Due to the issues described above, the ocean microstructure community was an early adopter of autonomous platforms

as observing tools, most notably in the form of large dropsonde-type profilers with simple weight release mechanisms that permit measurements to a predetermined depth. Such systems include the University of Washington Applied Physics Laboratory-designed Multi-Scale Profiler (Winkel et al., 1996) and the various versions of the Woods Hole Oceanographic Institution-designed High Resolution Profilers (Schmitt et al., 1988; St. Laurent et al., 2012). These systems are adept at achieving both very low noise levels (dissipation rates less than  $10^{-10} \text{ W kg}^{-1}$ ) and measurements to abyssal depths (to 6,000 m), but they require the costly time-consuming deck operations associated with the deployment and recovery of large autonomous instrumentation.

In all cases involving traditional sampling techniques, sea state and weather conditions are a major factor in collecting good-quality data. The deck operations of towed and tethered systems require manageable ship handling that varies by vessel but seldom permits sampling in conditions where winds exceed 40 knots. Autonomous profiler systems similarly require manageable sea states for deployment and recovery. Thus, there is a fair-weather bias to the existing microstructure database.

With the advancement of ocean autonomous systems over the last decade, a new platform has come to prominence with nearly ideal characteristics for microstructure sampling: undersea gliders. Driven by buoyancy-controlled flight, these systems are hydrodynamically very quiet. Moving parts are typically limited to an internal buoyancy pump and a pitch motor for altering the position of the battery, both of which can be restricted to operate at only the beginning and end of an ascent or descent. The only externally moving part of a Slocum glider is a small fin on the tail. With their long-persistence mission capability, gliders can ride out periods of rough seas, collecting data during times when ship-based operations would not be possible. There are numerous undersea gliders in commercial and

non-commercial production whose exact details vary, but their common characteristics make all versions worthy microstructure sampling platforms. As with all microstructure platforms, those systems with larger inertial mass are preferable, as this is the most effective way to damp platform-induced vibrational energy.

Here, we describe examples of novel microstructure measurements collected using the Slocum model of ocean glider, originally designed by Doug Webb of the Woods Hole Oceanographic Institution and currently manufactured by Teledyne Webb Research in Falmouth, Massachusetts. Slocum gliders have been in oceanographic use for over 15 years, and their engineering and science capabilities are described in the literature (e.g., Webb et al. 2001; Schofield et al., 2007). All gliders operate by adjusting their buoyancy to move down or up in the water column. Pitch is controlled by moving weight (the battery) fore and aft, changing the moment of inertia relative to the moment of buoyancy. As their names imply, gliders generate lift from their wings to translate vertical motion into lateral flight. On the Slocum platform, a rudder is used to achieve steering.

Our glider-based microstructure sampling capability is provided by a Slocum equipped with a Rockland Scientific Microrider (MR; Figure 1). The MR is a modular package that houses up to six microstructure probes. Internally, the MR chassis also houses a pressure sensor, inclinometers, and accelerometers. These sensors are used for motion analysis necessary for the processing of microstructure data. The MR is nearly neutrally buoyant; however, its placement on the dorsal part of the glider changes the axial moment of the system (also known as the H-moment), which is accounted for in the ballasting of the glider. The MR also adds about 30% more drag to the vehicle (proportional to the increased spatial area), and there is a corresponding decrease in the system's maximum speed of about 15%. Most significantly, the MR draws approximately 1 W while in operation,

more than double the hotel load of a standard Slocum running a CTD. In practice, the use of the MR reduces mission duration by about 25% relative to a system with no MR. Despite the penalties of drag and power draw, the addition of microstructure sensors adds a novel turbulence measurement capability that is unrivaled by other available sampling platforms.

## MICROSTRUCTURE SENSING FROM GLIDERS

As far as we are aware, the first deployment of a glider with microstructure sensing was in 2009 at the Ashumet Pond test site in Falmouth, Massachusetts. Wolk et al. (2009) describe data from that test, including demonstration of dissipation rate noise levels as low as  $5 \times 10^{-11} \text{ W kg}^{-1}$ , which is comparable to measurements achieved by the best untethered free-fall profilers. Subsequent early deployments of the system included numerous tests in US coastal waters.

The most sensitive issue involved in adapting the long-practiced techniques developed on towed systems and dropsondes to gliders is the computation of platform speed ( $V$ ). As Lueck (2003) discusses in detail,  $\epsilon \sim V^4$ . Thus, even a small error in speed translates to a large error

in dissipation rate. To explore the issues associated with estimating glider speed, a flight model must be invoked. The flight dynamics of ocean gliders have been the subject of many studies. One such study specific to the Slocum platform is that of Merckelbach et al. (2010). Gliders typically fly at a pitch angle of 25 to 30 degrees. Pitch, along with the rate of change of pressure (depth) are routinely measured by both the glider and separately at higher frequency by the MR package. The glider's speed is estimated using basic trigonometry as  $V = W/\sin(\gamma)$ , where  $V$  is the speed of the glider in the direction of glide,  $W$  is the vertical speed of the glider (as measured by the rate of change with pressure), and  $\gamma$  is the angle of glide. Complicating matters is the offset between the measured pitch angle ( $\phi$ ) and the angle of glide ( $\gamma$ ). These angles must have a small difference, as the difference between  $\phi$  and  $\gamma$  gives rise to hydrodynamic lift that allows the glider to "glide." This difference is the angle of attack ( $\alpha$ ).

Fer et al. (2014) studied the flight dynamics of the Slocum glider with the MR package. They find  $2^\circ < \alpha < 4^\circ$  as the consistent range of angles of attack for both diving and climbing during periods of stable flight (free ascent/descent



**FIGURE 1.** Photograph of the Teledyne Webb Research Slocum glider equipped with a Rockland Scientific Microrider (MR) package. The specialized probes for measuring microstructure are visible protruding past the nose of the instrument. *Photo courtesy of Ben Allsup*

periods during which the glider is not turning around at the top or bottom of a profile). The speed important to the microstructure measurement is the speed along the angle of glide ( $\gamma = \phi + \alpha$ ). The glider speed is estimated  $W/\sin(\phi + \alpha)$  as where  $W$  and  $\phi$  are measured values and  $\alpha = 3^\circ$  is assumed for angle of attack.

Figure 2 provides examples of microstructure shear spectra from the Slocum MR gliders we operate. These examples were collected as part of the Salinity Processes in the Upper-ocean Regional Study (SPURS, described in the following section). Spectra for dual shear probes are shown for two examples of

1 m (approximately 4 seconds each) records, both collected at roughly 50 m depth. In each case, a red and blue pair of spectra correspond to a shear variance measured from a pair of orthogonally mounted shear probes. These cases correspond to dissipation levels of approximately  $1.5 \times 10^{-7} \text{ W kg}^{-1}$  and  $8 \times 10^{-11} \text{ W kg}^{-1}$ , as measured by integrations of spectral variance for the mean of the signals from the two probes. The factor-of-two differences between the variance levels of the two probes is typical, and likely relates to issues associated with small amounts of vibrational energy manifesting in one probe more than the other,

or alternatively/additionally, small variations from the calibrated sensitivities of the probes due to biological films accumulating on the probe tips. In these cases where the signals are close, we simply take the mean. For lower levels of shear variance, as is the case for the  $8 \times 10^{-11} \text{ W kg}^{-1}$  example, vibrational energy coherent with the vehicle motion contaminates the spectra (thin red and blue lines), but is effectively removed by the Goodman et al. (2006) algorithm. Integration limits for each set of clean spectra, as derived from the roots of a fifth-order polynomial fit, are shown for each case.

### NEAR-SURFACE MEASUREMENTS OF TURBULENCE AND MIXING

Glidors are ideal platforms for sampling the surface layer of the ocean. Sampling away from the hull effects of ships or buoys, they provide measurements of undisturbed conditions. Also, in free ascent, a glider can sample microstructure up to the air-sea interface by breaching the surface. We deployed several MR gliders during SPURS in the North Atlantic, and also during the Bay of Bengal study known as ASIRI (Air-Sea Interaction Research Initiative). Figure 3 shows the locations of these glider measurements relative to the ocean basins in which they were operating.

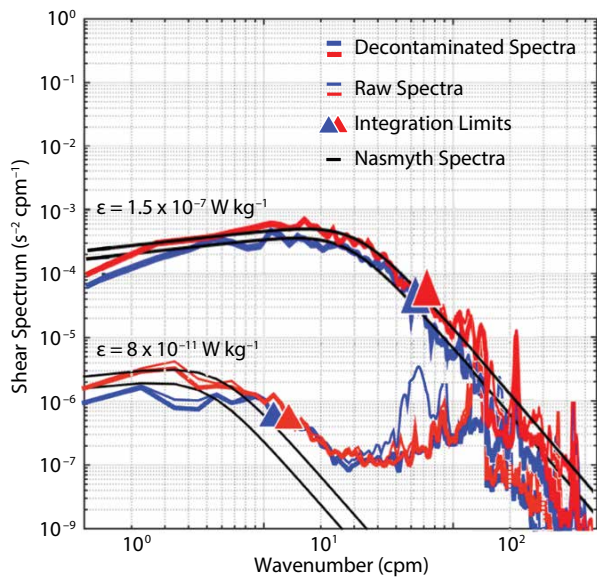


**FIGURE 2.** Examples of shear spectra from the MR glider operated during the 2012 Salinity Processes in the Upper Ocean Regional Study (SPURS) field program. Each set of spectra shows the shear variance as measured in a turbulent patch approximately 1 m in vertical scale at 50 m depth. Red and blue denote the independent signals of two probes whose deflection axes are at  $90^\circ$  offsets. The Nasmyth reference spectrum is shown for each case.

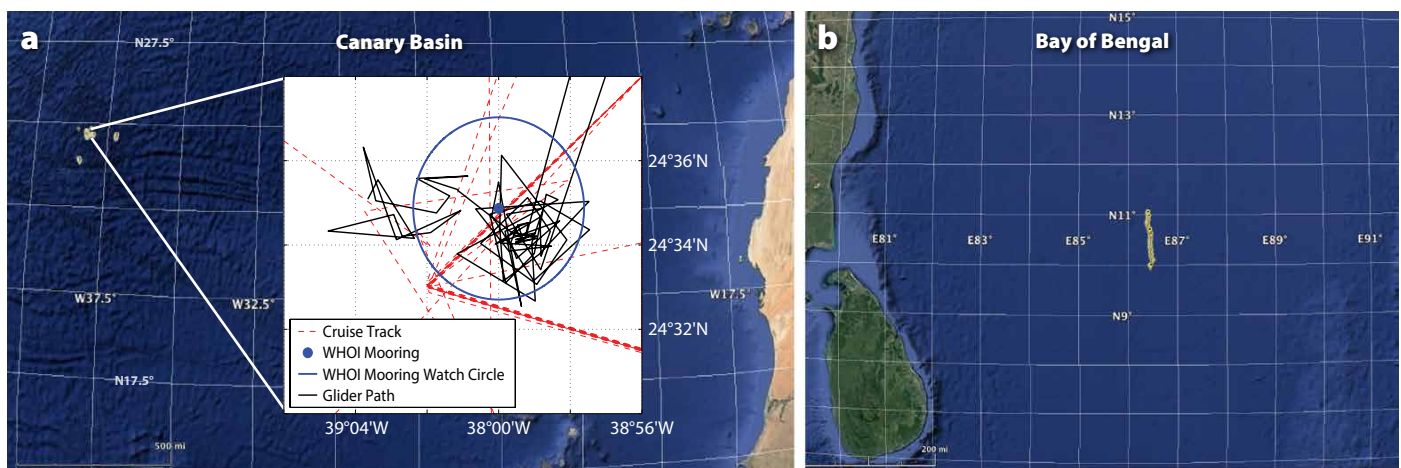


**FIGURE 3.** Maps showing the MR glider sampling locations for (a) the Salinity Processes in the Upper-ocean Regional Study (SPURS) program in the Canary Basin of the North Atlantic, and (b) the Air-Sea Interaction Research Initiative (ASIRI) study in the Bay of Bengal in the Indian Ocean. During SPURS, one MR glider sampled near an air-sea interaction buoy (located at  $24^\circ35'N$ ,  $38^\circ W$ ). The inset in panel a shows the detail of the glider occupation near the buoy. During ASIRI, the MR glider was used to sample a transect along  $86.5^\circ E$  between  $10^\circ N$  and  $11^\circ N$ .

### Stable Layers in the North Atlantic

During 2012 and 2013, we examined the turbulent properties of the near-surface layer as part of SPURS. This program was established to examine the cascade of processes that link the regional-scale salinity variance to the basin scale above, and the mesoscale below. The March 2015 issue of *Oceanography* (volume 28, issue 1) described the large observing effort during SPURS (Lindstrom et al., 2015). A central buoy with surface and subsurface instrumentation served as a focal point for intensive observations (Farrar et al., 2015), with numerous gliders sampling in close proximity (Figure 3a). Bogdanoff (2017) describes many additional details regarding the SPURS program and the MR glider components during the 2012 and 2013 observation periods.

Here, we describe a specific 12-day record of temperature, salinity, and turbulence dissipation rate collected using a Slocum flying an approximate 3 km watch circle around the SPURS buoy. These measurements were made between September 22 and October 4, 2012, corresponding to the initial phase of the overall SPURS program. Figure 4 shows the sea surface temperature (SST) and sea surface salinity (SSS) records as measured by the buoy, with nearby glider records of temperature and salinity.

Winds as measured at the buoy and the record of shortwave radiation are shown with the turbulent dissipation rate measurements and buoyancy gradient estimates in Figure 5. Winds decreased over the first week to less than  $0.5 \text{ m s}^{-1}$  (1 knot) on day 6 of the record (Figure 5a). For the first several days, the near-surface measurements of turbulent dissipation rate show a pattern of evening convection followed by daytime periods of restratification. This cycle has been previously described in earlier studies, notably by Moum et al. (1989) and Brainerd and Gregg (1993a,b).

During the fourth day of the glider mission, rainfall led to freshening of the surface waters, decreasing surface salinity (Figure 4). The wind dies down following

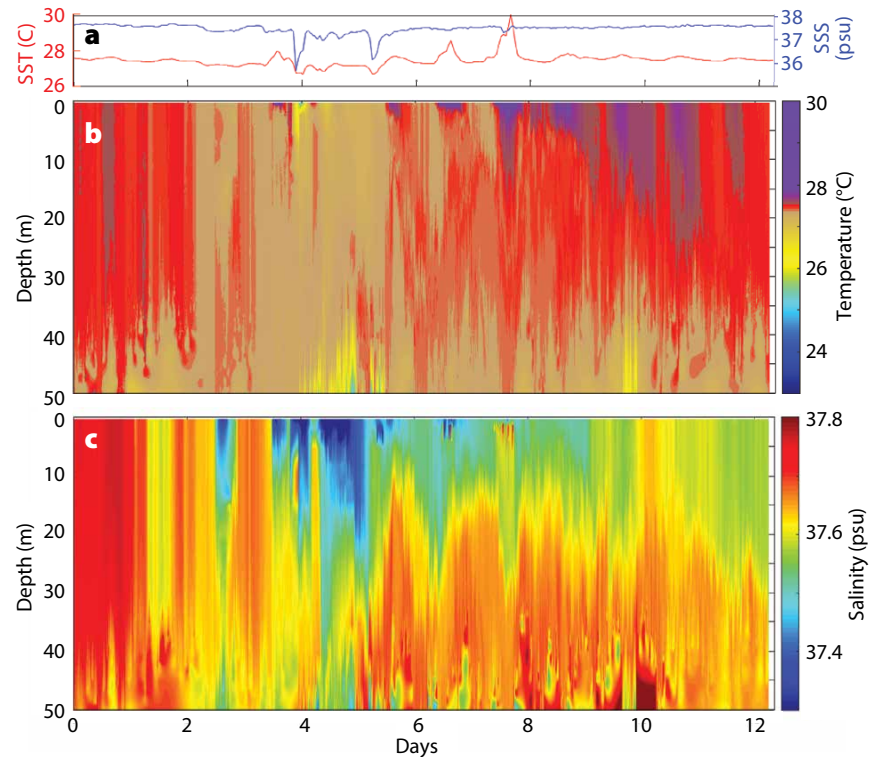


**FIGURE 4.** (a) Sea surface temperature (SST) and sea surface salinity (SSS) measured at the buoy for the time series corresponding to the nearby occupation of the MR glider during SPURS in 2012. (b) Temperature and (c) salinity for the upper 50 m measured by the MR glider, which flew within 3 km of the buoy during these 12 days.

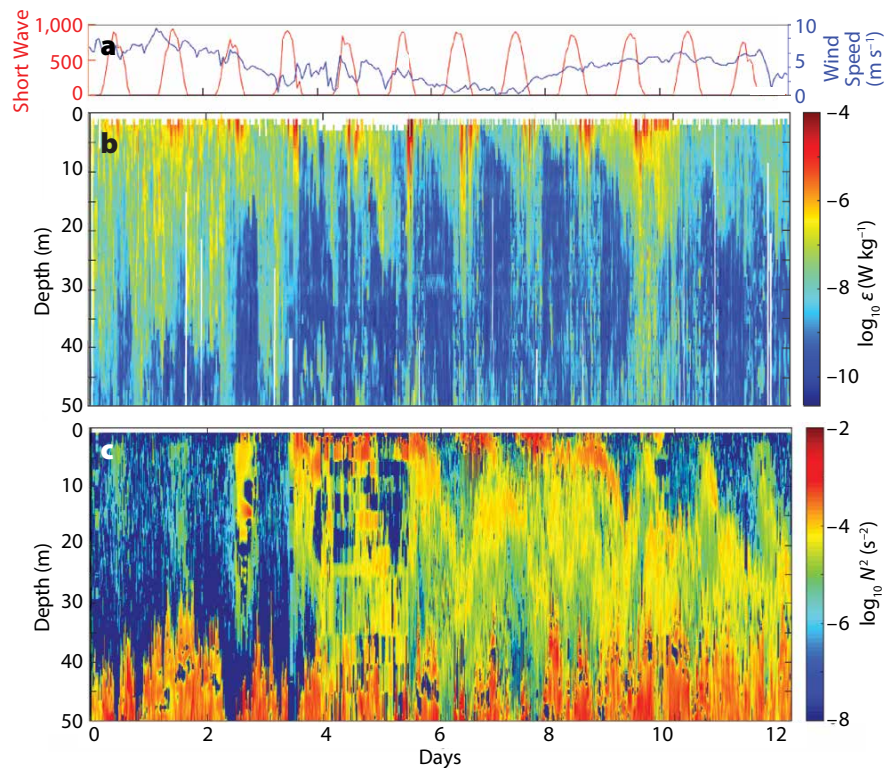


**FIGURE 5.** (a) Shortwave radiation and wind speed, as measured by the SPURS air-sea interaction buoy. (b) Turbulent kinetic energy dissipation rates, and (c) buoyancy gradient as measured by the MR glider.

this precipitation event, and the combination of the surface freshening and the reduction in winds triggers an interesting transition in the dissipation and stratification characteristics of the near-surface layer. Following day 4, the near-surface layer remains stratified even during the late evening hours. Moreover, a pattern of daily stable boundary layer formation is established, trapping turbulence levels

near the surface. The most notable daily SST modulations of 0.5°C, 1°C, and 2°C occur on days 5, 6, and 7 respectively, when the winds die to nearly zero.

Days 5, 6, and 7 are particularly interesting, as despite low winds, dissipation levels are maintained in a thin near-surface layer (Figure 6). The highest dissipation rates are observed during times of maximum insolation when

the near surface is significantly stratified. This surprising result is discussed in the next section, following Bogdanoff (2017), who found that the energy from the thermocline internal wave field resonates with the surface stable layer to drive shear and turbulence.

### Barrier Layers in the Bay of Bengal

Another interesting MR measurement in the ocean surface layer was collected in December 2013 in the central Bay of Bengal (BoB) along a meridional transect from 10°N to 11°N (Figure 3b) as part of the ASIRI study. The glider operated for seven days, collecting microstructure data in the upper 120 m of the water column. The goal of the survey was to observe water mass structure and quantify turbulence and mixing rates in the near-surface layer. The glider observations were collected as part of a larger program involving research expeditions by the Indian ORV *Sagar Nidhi*, the Sri Lankan R/V *Samudrika*, and the US R/V *Roger Revelle*. Additional aspects of ASIRI are described by Mahadevan et al. (2016), and in the numerous papers of the June 2016 issue (volume 29, issue 2) of *Oceanography*. As far as we know, these were among the first direct measurements of turbulence in the BoB. The glider transect was obtained simultaneously with ship-based profiling measurements of microstructure reported by Jinadasa et al. (2016). Detailed measurements of air-sea fluxes and features of the near-surface turbulence were measured at a buoy at 18°N (Weller et al., 2016), and temperature measurements made from a nearby profiling float were used to derive mixing levels (Shroyer et al., 2016).

Large amounts of freshwater (riverine inflow and precipitation) influence stratification in the BoB (Figure 7), resulting in a highly stable stratified layer below the surface turbulent layer. This “barrier layer” (Agarwal et al., 2012; Shroyer et al., 2016) traps wind and wave energy to the near surface. While we do not have direct observations of wind and waves along the glider transect, meteorological data

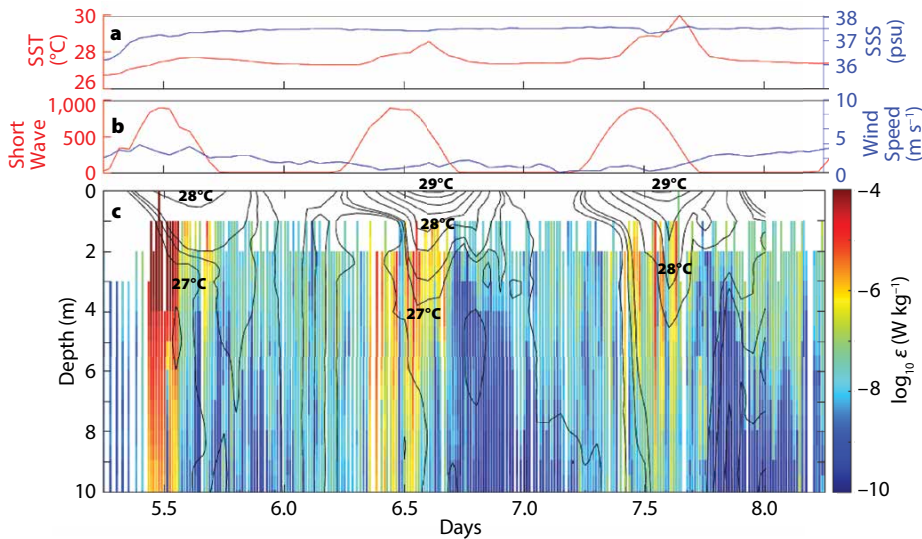


**FIGURE 6.** (a) SST and SSS, and (b) shortwave radiation and wind speed from the SPURS buoy for the three-day period when stable layers formed at the surface. (c) Dissipation rates and temperature as measured by the MR glider. Dissipation estimates are done for 1 m bins, as described in the text.

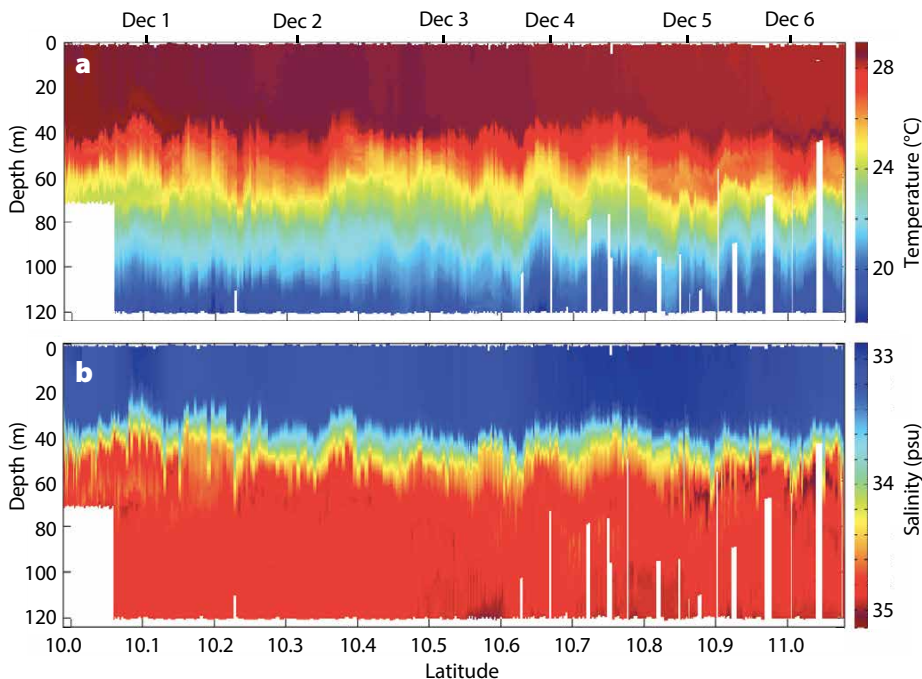


**FIGURE 7.** (a) Temperature and (b) salinity from the MR glider deployed in the Bay of Bengal during the ASIRI study. Dates (UTC) are shown along the upper axis.

subsampled from the European Centre for Medium-Range Weather Forecasts (ECMWF) indicate that wind speeds were between  $5 \text{ m s}^{-1}$  and  $10 \text{ m s}^{-1}$  (Figure 8a).

Figure 8b,c also shows turbulent dissipation rates and buoyancy frequency. Dissipation rates change dramatically across the layer, ranging from  $1 \times 10^{-5} \text{ W kg}^{-1}$  above the barrier layer to  $1 \times 10^{-10} \text{ W kg}^{-1}$  below it (Figure 8b). The  $N^2$  section (Figure 8c) suggests that at the time of measurements, the barrier layer resides at about 40 m depth with values reaching  $1 \times 10^{-3} \text{ s}^{-2}$ , separating a weakly stratified near-surface layer from the pycnocline below. The dissipation rate above the barrier is typical of open-ocean active boundary layers where meteorological forcing energizes strong turbulence. The physics of such turbulence is generally well described by the log-layer model of a sheared boundary layer (e.g., Brainerd and Gregg 1993a, 1993b). The weak dissipation-rate values below the barrier are typical of the low-latitude thermocline, where the background internal wave field (e.g., Munk, 1981) supports intermittent shear-driven turbulence.

While Shroyer et al. (2016) document turbulence levels modulated by diurnal convection at the buoy site at  $18^\circ\text{N}$ , we do not see clear evidence of diurnal processes in the glider data. It is possible that in the central BoB at  $10^\circ\text{N}$ – $11^\circ\text{N}$ , the diurnal cycle was much weaker than that in the northern BoB at  $18^\circ\text{N}$ .

Given the relatively stable conditions in winds and hydrography along our section, it is possible to use all 390 profiles of dissipation rates and stratification to derive a meaningful mean profile (Figure 9a). A decrease in turbulence levels is clearly apparent between 40 m and 60 m depth. This mean dissipation profile can be used to calculate a profile of diffusivity via the model proposed by Osborn (1980),  $k_p = \Gamma \langle \epsilon \rangle / \langle N^2 \rangle$ , where  $\Gamma$  is a parameter related to the mixing efficiency, and is assumed to have the value of 0.2. Figure 9b shows the vertical diffusivity estimate derived from the mean

profile of dissipation rate and the mean profile of buoyancy gradient. The role of stratification makes for an extremely abrupt change in mixing levels across the barrier. Our result here is consistent with that of Jinadasa et al. (2016), who also document an abrupt decrease in the dissipation rate beneath the barrier layer at other sites in the BoB.

## DISCUSSION

This study focused on two cases where surface buoyancy forcing profoundly influenced stratification and turbulence in the upper ocean. In the subtropical Atlantic (the SPURS region), atmospheric heating acts to stratify the upper few meters of the ocean during periods of weak winds. The effect is more pronounced when the sea surface is freshened by heavy rainfalls preceding heating periods. In the Bay of Bengal, salinity also plays the key role in the formation of a barrier layer, which separated the surface mixing layer from the weakly turbulent pycnocline.

Measurements in the Atlantic show that the enhanced near-surface stratification appears to increase near-surface

turbulence during very quiet atmospheric conditions. This turbulence could be induced by instability of an internal wave mode of the stable layer that resonates with the internal wave energy of the thermocline. D'Asaro (1978) first predicted this mode of resonance, theoretically linking the velocities of the deep internal wave field with that of a surface mixed layer. Resonance occurs under certain conditions when the wavelength content of the deep internal waves matches a scaled relationship with the thickness of the surface layer, with the scaling dependent on the stratification parameters. Bogdanoff (2017) extended the D'Asaro framework to apply to the stable layer scenario, in which the thin stable layer assumes the role of the mixed layer in D'Asaro's model. Bogdanoff (2017) carefully considered the conditions applicable to the stable layer scenarios observed during SPURS, and found that the resonance condition likely occurs. This assertion is supported by the observations of Hodges and Fratantoni (2014), who directly observed an internal wave mode of the stable layer at the SPURS site during the period of our

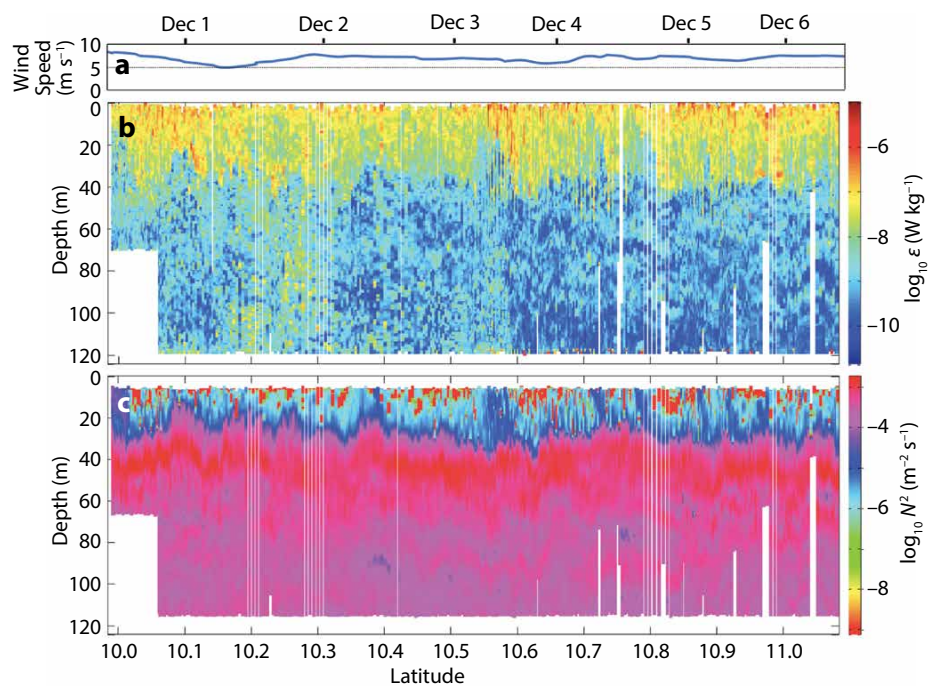


**FIGURE 8.** (a) ECMWF winds reconstructed for the spatial section occupied by the MR glider. (b) Dissipation rate and (c) buoyancy gradient as measured by the glider between  $10^\circ\text{N}$  and  $11^\circ\text{N}$ . Dates (UTC) are shown along the upper axis.

glider observations. Bogdanoff (2017) concludes that instability of the stable layer internal-wave mode is the only mechanism capable of supporting the turbulent dissipation rate levels measured by the glider.

In the BoB, the warm, low-saline surface water overlying the cooler, saltier water below gives rise to a strongly stratified “barrier layer.” During November and December of 2013, various ship-based surveys (Jinadasa et al., 2016), profiling float observations (Shroyer et al., 2016), and our glider transect observed a 10 m to 20 m thick barrier layer centered between 30 m and 40 m depth to be a widespread characteristic of the western BoB, spanning the meridional extent of the basin. These studies derived estimates of turbulent dissipation levels using various methodologies, and found that the presence of a barrier layer provided a striking contrast between the energetic turbulence levels of the near surface and quiescent waters below. Though the barrier layer was expected to provide such a contrast (as its name implies), the level of quiescence below, particularly as measured by diffusivity (Figure 8b), is surprising. Typical mid-latitude regions of the ocean are characterized by thermocline mixing levels of  $1 \times 10^{-5} \text{ m}^2 \text{ s}^{-1}$ , whereas our data indicate mixing rates an order of magnitude less. These values suggest that the internal wave climate of the BoB might be less energetic than comparable

regions of other ocean basins. A potential explanation for the low values may be that the barrier layer inhibits the transfer of wind energy (mostly in the inertial band) into the deep internal wave field. Additionally, the energy of the deep internal wave field may be modulated by the monsoon cycle. Such questions will be fruitful pursuits in the upcoming international field effort known as MISO-BoB (Monsoon Intra-Seasonal Oscillations in the Bay of Bengal) planned for 2018 and 2019. Glider-based measurements of microstructure are planned for both phases of the monsoon cycle, and during the intermonsoon period.

The era of glider-based microstructure sampling, and autonomous platform-based microstructure sampling is at its beginning. Several dozen Slocum-model gliders outfitted with microstructure sensing are currently in use throughout the oceanographic community. The Seaglider, developed by the University of Washington and now manufactured by Kongsberg Marine, also has a newly developed microstructure sensing payload. The long-persistence mission capabilities of Seaglider will provide new scientific possibilities for microstructure sampling and also new challenges, as probe longevity may become a limiting factor. The new version of the Seaglider, known as Deepglider, is a 6,000 m depth capable glider system also capable of microstructure sampling. Deepglider,

along with the Sea Explorer glider model of the French company Alseamar, are the first glider designs built to handle microstructure sensing as a payload option integrated into the vehicle nose.

Many other innovations are in the works for glider microstructure sensing. New microstructure-band velocity sensors (such as those from Alec Electronics and Nortek) are being used to directly measure flow past the nose of the glider during flight. These measurements solve the angle-of-attack problem described previously, as the glider speed is measured directly. Furthermore, the use of high-frequency acoustic Doppler velocimeters (such as the Nortek ADV sensor) have enabled some users to estimate the turbulent dissipation rate through measuring the inertial subrange of the velocity spectrum (Emily Shroyer, Oregon State University, *pers. comm.*, 2017). Newer model glider systems also feature thrusters (on Slocum G2 and G3 models) and larger volume buoyancy ballast systems (1,000 cc for the Slocum G3). Both of these innovations permit increased speed during flight, allowing a glider to fly through stronger currents, or sample a spatial region faster, potentially avoiding aliasing of temporal signals.

Research groups at the University of Washington Applied Physics Laboratory and the Woods Hole Oceanographic Institution have developed onboard microstructure processing capabilities for Seaglider (Rainville et al., 2017, in this issue) and Slocum, respectively. These units permit the transmission of turbulent dissipation rate estimates via Iridium satellite communications. The operator gains the value of having these data returned prior to the glider being recovered (especially valuable if the glider is lost). The operator also gains the value of using these data to modify a mission plan. For example, the mission might be modified to concentrate measurements in a depth range where turbulence is enhanced, or the timing of surface intervals might be modified to better resolve a temporal cycle of turbulence. These innovations

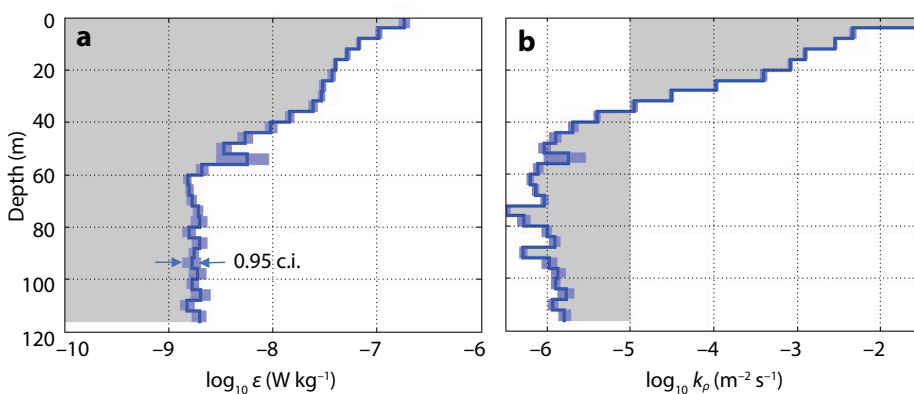


**FIGURE 9.** (a) Mean profile computed from the 390 measured profiles of dissipation rate. The shaded scaling about the binned means indicated the 95% confidence intervals. (b) A profile of diffusivity derived from mean dissipation profile, the mean buoyancy gradient, and an assumed mixing efficiency of 20%.

will revolutionize the study of ocean mixing, making what has been a traditionally very sparse form of ocean data something that is routinely sampled. 

## REFERENCES

- Agarwal, N., R. Sharma, A. Parekh, S. Basu, A. Sarkar, and V.K. Agarwal. 2012. Argo observations of barrier layer in the tropical Indian Ocean. *Advances in Space Research* 50(5):642–654, <https://doi.org/10.1016/j.asr.2012.05.021>.
- Bogdanoff, A.S. 2017. *Physics of Diurnal Warm Layers: Turbulence, Internal Waves, and Lateral Mixing*. Doctoral dissertation, Massachusetts Institute of Technology.
- Brainerd, K.E., and M.C. Gregg. 1993a. Diurnal restratification and turbulence in the oceanic surface mixed layer: 1. Observations. *Journal of Geophysical Research* 98(C12):22,645–22,656, <https://doi.org/10.1029/93JC02297>.
- Brainerd, K.E., and M.C. Gregg. 1993b. Diurnal restratification and turbulence in the oceanic surface mixed layer: 2. Modeling. *Journal of Geophysical Research* 98(C12):22,657–22,664, <https://doi.org/10.1029/93JC02298>.
- D'Asaro, E.A. 1978. Mixed layer velocities induced by internal waves. *Journal of Geophysical Research* 83(C5):2,437–2,438, <https://doi.org/10.1029/JC083iC05p02437>.
- Dillon, T.M., J.A. Barth, A.Y. Erofeev, G.H. May, and H.W. Wijesekera. 2003. MicroSoar: A new instrument for measuring microscale turbulence from rapidly moving submerged platforms. *Journal of Atmospheric and Oceanic Technology* 20(11):1,671–1,684, [https://doi.org/10.1175/1520-0426\(2003\)020<1671:MANIFM>2.0.CO;2](https://doi.org/10.1175/1520-0426(2003)020<1671:MANIFM>2.0.CO;2).
- Goodman, L., E.R. Levine, and R.G. Lueck. 2006. On measuring the terms of the turbulent kinetic energy budget from an AUV. *Journal of Atmospheric and Oceanic Technology* 23(7):977–990, <https://doi.org/10.1175/JTECH18891>.
- Farrar, J.T., L. Rainville, A.J. Plueddemann, W.S. Kessler, C. Lee, B.A. Hodges, and D.M. Fratantoni. 2015. Salinity and temperature balances at the SPURS central mooring during fall and winter. *Oceanography* 28(1):56–65, <https://doi.org/10.5670/oceanog.2015.06>.
- Fer, I., A.K. Peterson, and J.E. Ullgren. 2014. Microstructure measurements from an underwater glider in the turbulent Faroe Bank Channel overflow. *Journal of Atmospheric and Oceanic Technology* 31(5):1,128–1,150, <https://doi.org/10.1175/JTECH-D-13-00221.1>.
- Grant, H.L., R.W. Stewart, and A. Moilliet. 1962. Turbulence spectra from a tidal channel. *Journal of Fluid Mechanics* 12(2):241–268, <https://doi.org/10.1017/S002211206200018X>.
- Gregg, M.C. 1999. Uncertainties and limitations in measuring  $\epsilon$  and  $\chi$  T. *Journal of Atmospheric and Oceanic Technology* 16(11):1,483–1,490, [https://doi.org/10.1175/1520-0426\(1999\)016<1483:UALIMA>2.0.CO;2](https://doi.org/10.1175/1520-0426(1999)016<1483:UALIMA>2.0.CO;2).
- Hinze, J.O. 1975. *Turbulence*, 2<sup>nd</sup> ed. McGraw-Hill, 790 pp.
- Hodges, B.A., and D.M. Fratantoni. 2014. AUV observations of the diurnal surface layer in the North Atlantic salinity maximum. *Journal of Physical Oceanography* 44:1,595–1,604, <https://doi.org/10.1175/JPO-D-13-0140.1>.
- Jinadasa, S.U.P., I. Lozovatsky, J. Planella-Morató, J.D. Nash, J.A. MacKinnon, A.J. Lucas, and H.J. Fernando. 2016. Ocean turbulence and mixing around Sri Lanka and in adjacent waters of the northern Bay of Bengal. *Oceanography* 29(2):170–179, <https://doi.org/10.5670/oceanog.2016.49>.
- Kunze, E., M.G. Briscoe, and A. Williams. 1990. Interpreting shear and strain fine structure from a neutrally buoyant float. *Journal of Geophysical Research* 95:18,111–18,125, <https://doi.org/10.1029/JC095iC10p18111>.
- Lindstrom, E., F. Bryan, and R. Schmitt. 2015. SPURS: Salinity Processes in the Upper-Ocean Regional Study—The North Atlantic Experiment. *Oceanography* 28(1):14–19, <https://doi.org/10.5670/oceanog.2015.01>.
- Lueck, R. 2003. Rockland Scientific Technical Note 28. <http://www.rocklandscientific.com>.
- Lueck, R.G., F. Wolk, and H. Yamazaki. 2002. Oceanic velocity microstructure measurements in the 20th century. *Journal of Oceanography* 58(1):153–174, <https://doi.org/10.1023/A:1015837020019>.
- Mahadevan, A., G.S. Jaeger, M. Freilich, M.M. Omand, E.L. Shroyer, and D. Sengupta. 2016. Freshwater in the Bay of Bengal: Its fate and role in air-sea heat exchange. *Oceanography* 29(2):72–81, <https://doi.org/10.5670/oceanog.2016.40>.
- Mater, B.D., S.K. Venayagamoorthy, L. St. Laurent, and J.N. Moum. 2015. Biases in Thorpe-scale estimates of turbulence dissipation: Part I. Assessments from large-scale overturns in oceanographic data. *Journal of Physical Oceanography* 45(10):2,497–2,521, <https://doi.org/10.1175/JPO-D-14-0128.1>.
- Merkelbach, L., D. Smeed, and G. Griffiths. 2010. Vertical water velocities from underwater gliders. *Journal of Atmospheric and Oceanic Technology* 27:547–563, <https://doi.org/10.1175/2009JTECHO710.1>.
- Moum, J.N., D.R. Caldwell, and C.A. Paulson. 1989. Mixing in the equatorial surface layer and thermocline. *Journal of Geophysical Research* 94(C2):2,005–2,022, <https://doi.org/10.1029/JC094iC02p02005>.
- Munk, W. 1981. Internal waves and small-scale mixing processes. Pp. 264–290 in *Evolution of Physical Oceanography*. B.A. Warren and C. Wunsch, eds, MIT Press.
- Nasmyth, P.W. 1970. *Oceanic Turbulence*. Doctoral dissertation, University of British Columbia.
- Osborn, T.R. 1980. Estimates of the local rate of vertical diffusion from dissipation measurements. *Journal of Physical Oceanography* 10(1):83–89, [https://doi.org/10.1175/1520-0485\(1980\)010<0083:EOTLRO>2.0.CO;2](https://doi.org/10.1175/1520-0485(1980)010<0083:EOTLRO>2.0.CO;2).
- Paka, V.T., V.N. Nabatov, I.D. Lozovatsky, and T.M. Dillon. 1999. Oceanic microstructure measurements by BAKLAN and GRIF. *Journal of Atmospheric and Oceanic Technology* 16(11):1,519–1,532, [https://doi.org/10.1175/1520-0426\(1999\)016<1519:OMMBBA>2.0.CO;2](https://doi.org/10.1175/1520-0426(1999)016<1519:OMMBBA>2.0.CO;2).
- Rainville, L., J.I. Gobat, C.M. Lee, and G.B. Shilling. 2017. Multi-month dissipation estimates using microstructure from autonomous underwater gliders. *Oceanography* 30(2):49–50, <https://doi.org/10.5670/oceanog.2017.219>.
- Schmitt, R.W., J.M. Toole, R.L. Koehler, E.C. Mellinger, and K.W. Doherty. 1988. The development of a fine- and microstructure profiler. *Journal of Atmospheric and Oceanic Technology* 5(4):484–500, [https://doi.org/10.1175/1520-0426\(1988\)005<0484:TDOAFA>2.0.CO;2](https://doi.org/10.1175/1520-0426(1988)005<0484:TDOAFA>2.0.CO;2).
- Schofield, O., J. Kohut, D. Aragon, L. Creed, J. Graver, C. Haldeman, J. Kerfoot, H. Roarty, C. Jones, D. Webb, and S. Glenn. 2007. Slocum gliders: Robust and ready. *Journal of Field Robotics* 24(6):473–485, <https://doi.org/10.1002/rob.20200>.
- Shroyer, E.L., D.L. Rudnick, J.T. Farrar, B. Lim, S.K. Venayagamoorthy, L. St. Laurent, and J.N. Moum. 2016. Modification of upper-ocean temperature structure by subsurface mixing in the presence of strong salinity stratification. *Oceanography* 29(2):62–71, <https://doi.org/10.5670/oceanog.2016.39>.
- St. Laurent, L., A.C. Naveira Garabato, J.R. Ledwell, A.M. Thurnherr, J.M. Toole, and A.J. Watson. 2012. Turbulence and diapycnal mixing in Drake Passage. *Journal of Physical Oceanography* 42:2,143–2,152, <https://doi.org/10.1175/JPO-D-12-027.1>.
- Thorpe, S.A. 1977. Turbulence and mixing in a Scottish loch. *Philosophical Transactions of the Royal Society of London A* 286(1334):125–181, <https://doi.org/10.1098/rsta.1977.0112>.
- Thorpe, S. 2007. *An Introduction to Ocean Turbulence*. Cambridge University Press, 267 pp.
- Webb, D.C., P.J. Simonetti, and C.P. Jones. 2001. SLOCUM: An underwater glider propelled by environmental energy. *IEEE Journal of Oceanic Engineering* 26(4):447–452, <https://doi.org/10.1109/48.972077>.
- Weller, R.A., J.T. Farrar, J. Buckley, S. Mathew, R. Venkatesan, J.S. Lekha, and B.P. Kumar. 2016. Air-sea interaction in the Bay of Bengal. *Oceanography* 29(2):28–37, <https://doi.org/10.5670/oceanog.2016.36>.
- Winkel, D.P., M.C. Gregg, and T.B. Sanford. 1996. Resolving oceanic shear and velocity with the Multi-Scale Profiler. *Journal of Atmospheric and Oceanic Technology* 13:1,046–1,073, [https://doi.org/10.1175/1520-0426\(1996\)013<1046:ROSAVW>2.0.CO;2](https://doi.org/10.1175/1520-0426(1996)013<1046:ROSAVW>2.0.CO;2).
- Wolk, F., R.G. Lueck, and L. St. Laurent. 2009. Turbulence measurements from a glider. Pp. 1–6 in *OCEANS 2009, MTS/IEEE Biloxi - Marine Technology for Our Future: Global and Local Challenges*. October 26–29, 2009.

## ACKNOWLEDGMENTS

We thank the US Office of Naval Research (ONR) for supporting the development of autonomous glider systems and the integration effort to incorporate microstructure sensing. The National Science Foundation supported the SPURS microstructure glider effort. ONR supported for the glider program in the Bay of Bengal. Despite a common claim that glider-based measurements have somehow lessened the dependence on technical personnel, the reality is that many people support these sophisticated autonomous platforms both in the field and behind the scenes. We are grateful for the efforts of many outstanding colleagues who made the glider observations we presented possible. In particular, we thank Alec Bogdanoff, Ken Decoteau, Jim Riley, Oliver Sun, and Sean Whelan for their significant efforts in the field programs described in this manuscript. We additionally thank Lou Goodman, Rolf Lueck, and Fabian Wolk for long collaborative partnerships that influenced many aspects of our work.

## AUTHORS

**Louis St. Laurent** (lstlaurent@whoi.edu) is Senior Scientist, Woods Hole Oceanographic Institution, Woods Hole, MA, USA. **Sophia Merrifield** is Postdoctoral Fellow, Scripps Institution of Oceanography, University of California, San Diego, La Jolla, CA, USA.

## ARTICLE CITATION

St. Laurent, L., and S. Merrifield. 2017. Measurements of near-surface turbulence and mixing from autonomous ocean gliders. *Oceanography* 30(2):116–125, <https://doi.org/10.5670/oceanog.2017.231>.